Research Journal of Chemical Sciences _____ ISSN 2231-606X
Vol. **5(3),** 1-5, March **(2015)** *Res. J. Chem. Sci.*

Structural, Optical and Dielectric Properties of Tin Selenide Nanoparticles Prepared by Aqueous Solution Method

Solanki G. K.[1]*, Gosai N.N.[2] and Patel K.D.[1]
[1]Department of Physics, Sardar Patel University, Vallabh vidyanagar 388 120, Gujarat, INDIA
[2]Department of Physics, Matushri Virbaima Mahila Science & Home Science College, Rajkot, Gujarat, INDIA

Available online at: www.isca.in, www.isca.me
Received 12th July 2014, revised 2nd March 2015, accepted 16th March 2015

Abstract

The present research paper reports the preparation and characterization of nano particles of Tin Selenide (SnSe) by chemical precipitation method in deionized water. Chemical composition of grown powder is studied with the help of EDAX. Nanostructures of the prepared SnSe particles have been characterized through XRD, TEM, UV-VIS-NIR spectroscopy techniques. The X-ray diffraction studies indicated the formation of SnSe nanoparticles with orthorhombic phase and average particle size determined by Scherrer's formula has been found to be 9.96 nm suggesting the formation of SnSe quantum dots. The prepared nanostructures have been also analyzed by TEM. The value of the measured optical band gap has been utilized to calculate the particle size (10.13 nm). Dielectric properties of tin selenide nano particles are investigated. It showed strong frequency and temperature dependence of capacitance, dielectric loss, real and imaginary part of dielectric constant over the frequency and temperature ranges of 100Hz- 1MHz and 300-420 K, respectively.

Keywords: SnSe quantum dots, quantum confinement effect, aqueous solution method, EDAX, XRD, TEM and UV VIS NIR spectrophotometry and dielectric properties of SnSe nanoparticles.

Introduction

Due to Nanoparticle's unique chemical, physical, optical, dielectrical and electrical transport properties which are different from those of either the bulk materials or single atom[1,2] as well as due to the vast surface area, all nanostructured materials posses a huge surface energy. In fabrication and processing of nanomaterials, to overcome the surface energy and to prevent the nanomaterials from growth in size can be driven by the reduction of overall surface energy. Semiconductor nanoparticles exhibit size-dependent properties which are presented by many researchers[3-9].

Tin Selenide (SnSe), a member of group IV-VI semiconductors is one of the promising materials from its applications point of view. SnSe in bulk crystalline and thin film form has been used as memory switching devices, holographic recording systems, and infrared electronic devices[10,11]. SnSe nanoparticles were synthesized by several methods like solid-state reaction, solid-state metathesis, Bridgman method, self-propagating high-temperature synthesis and brush plating technique[12-16]. Generally, these methods have some limitations; e.g. the requirement of a special device, toxic reagents and high processing temperature etc. Recently, solution routes, such as hydrothermal, solvothermal and organometallic precursor methods[17-19] have been developed for the synthesis of SnSe nanoparticles. In this reported work, synthesis of SnSe nanoparticles without using any capping agent by ordinary chemical precipitation synthesis route at room temperature.

Material and Methods

Chemicals in this synthesis process were of analytical reagent (AR) grade (99.99% purity, Alpha essar). Aqueous solutions of $SnCl_2$ (0.1M) and SeO_2 (0.1M) were used as the sources of Sn and Se, respectively. The $SnCl_2$ and SeO_2 solutions were mixed for 30 min using a magnetic stirrer by drop wise and as a result precipitations of SnSe were obtained in a solution. This precipitate was centrifuged at 3000 rpm for 15 min for separation of SnSe nanoparticles. Finally separated nanoparticles were washed by methanol several times and kept at 300°C for 1h in order to remove residual organic and inorganic solvent for obtaining dry powder of SnSe nanoparticles. Compositional study of as synthesized nanoparticles was carried out by EDAX (Philips, XL 30 ESEM). The structural characterization of grown powder was carried out by analyzing the XRD pattern (powder diffractometer-Philips 'X' PERT MPD' with CuKα = 1.5406 Å radiation). Particle size determination was confirmed by Transmission Electron Microscope (TEM).

Optical absorption spectroscopy measurements were carried out in the wave length range 200nm to 2500nm (Perkin Elmer Lambda-19). The prepared nanoparticles were compressed at 10 MPa in order to have pellet of the thickness 0.41cm and area 0.074cm^2 for dielectric measurements. Dielectric properties were measured with the help of HP4284A LCR meter along with an ON-OFF type temperature controller in the temperature range 300K to 420 K and in the frequency range 100 Hz to 1 MHz.

The basic measurements were carried out for capacitance (C) and dielectric loss (D) at different frequency and temperature by a suitable LabView programme. This basic measurands were then used to calculate real and imaginary part of dielectric constant.

Results and Discussion

EDAX: Figure 1 shows EDAX Spectrum of SnSe nanoparticles. The stoichiometric proportion of the constituent elements obtained from EDAX and expected values are nearly matching as given in table-1. The observed variation in stoichiometry is due to environmental processing of chemicals e.g. precipitation, centrifuge and annealing.

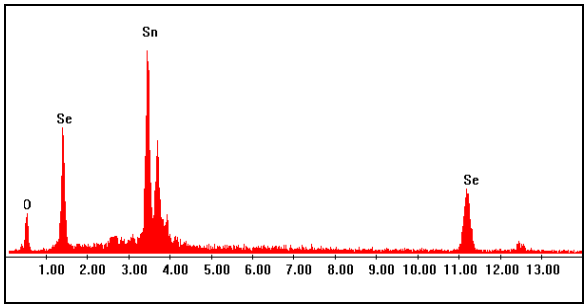

Figure-1
EDAX spectrum of prepared SnSe nanoparticles

Table-1
Elemental proportion of Sn and Se in SnSe nanoparticles as determined by EDAX

Elements	Wt (%) obtain from EDAX	Wt (%) calculated by theoretical
Sn	55.45	60.05
Se	34.89	39.95

XRD: Crystalline phase of the nanoparticles as well as the crystallite size can be obtained from XRD pattern.

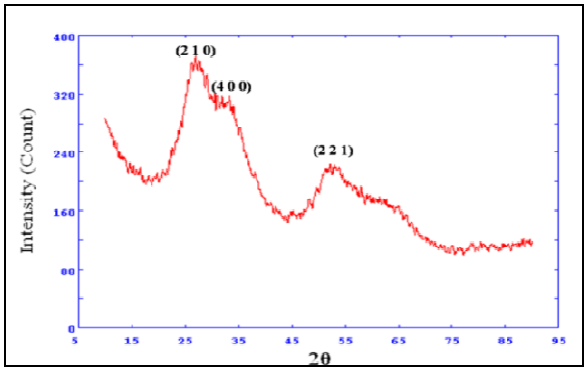

Figure-2
XRD pattern of prepared SnSe nanoparticles

Figure-2 shows the x-ray diffraction pattern of SnSe nanoparticles prepared by chemical precipitation method. The x-ray diffraction pattern exhibit peaks at 26.62°,31.35° and 50.66° corresponding to the (210), (400) and (221) planes. All these peaks correspond to the orthorhombic phase. The lattice parameter values a, b and c have been calculated and are found to be a = 11.41Å, b = 4.21Å and c = 4.30 Å which are in good agreement with the JCPDS data (card no. 321382). The presence of small and broad peaks in the x-ray diffractogram reveals the formation of nanoparticles. The broaden peaks indicating or presenting average crystallite size is small.

Based on size effect, peaks in the X – ray diffraction pattern broaden and their widths become large as the particles become smaller. The average size of particles has been obtained from the x-ray diffraction pattern using the Scherrer's formula[20].

$$D = \frac{K\lambda}{\beta\cos\theta} \quad (1)$$

Where: D is the grain size, K is a constant taken to be 0.94, β is the full width at half maximum (FWHM) and λ is the wave length of the x-rays (1.5406Å). The obtained average particle size of the prepared SnSe nanoparticles is 9.96nm. Our experimentally obtained data imply that the average radius of SnSe nanoparticle is smaller than the Bohr excitonic radius (r_B) for this material. This is a condition which has to be fulfilled in order to observe the quantum confinement effects. The Bohr excitonic radius r_B for a bulk semiconducting material is given by[21].

$$r_B = \frac{4\pi\pi_0\varepsilon_r\hbar^2}{e^2 m_0}\left(\frac{1}{m_e^*}+\frac{1}{m_h^*}\right) \quad (2)$$

Where symbols have their usual meaning. This quantum confinement has also been confirmed by TEM and UV-VIS-NIR spectroscopy.

The amorphous nature as depicted by the XRD pattern shown in the Figure 2 is due to the aqueous reaction medium that is responsible for uncontrolled nucleation of SnSe. On the other hand it is observed that the alkaline medium allows slow and controlled nucleation resulting in to more oriented and crystalline nature of nanomaterials[22].

TEM: The TEM micrograph as obtained in the image mode gives the morphology of the nanoparticles.

Figure-3 shows that nanoparticles of SnSe are homogeneous and spherical. This type of agglomerate nature of grown nanoparticles was also observed by other workers[23]. The particle size of these nanoparticles vary from 7.58 - 11.45 nm, and the average diameter of these nanoparticles is about 8.63nm.

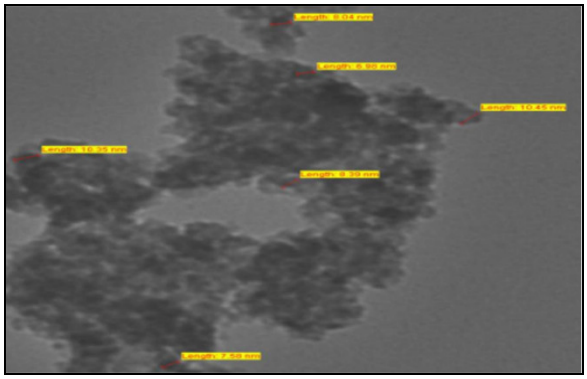

Figure-3
TEM photograph of prepared SnSe nanoparticles

UV-VIS-NIR: From the transmission data, the absorption coefficient (α) is calculated using the relation

$$\alpha = \frac{1}{d} \ln \left(\frac{1}{T} \right) \quad (3)$$

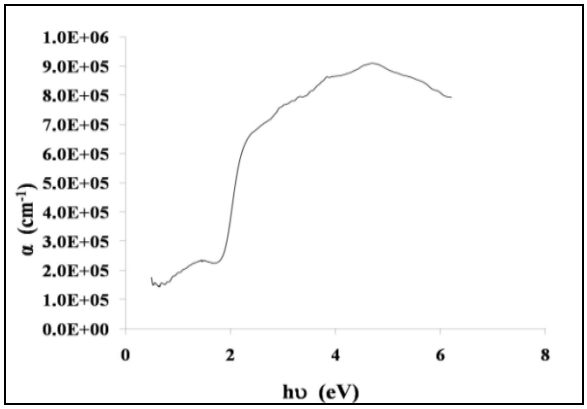

Figure 4
Plot of α vs hυ for prepared SnSe nanoparticles

Figure-4 shows the plot of α→ photon energy (hυ) where the fundamental absorption edge corresponding to the transition from valence band to the conduction band is clearly visible at photon energy of around 2.00 eV. This can be used to determine the band gap of the material using the relation[24].

$$\alpha h \upsilon = A \left(h\upsilon - E_g \right)^r \quad (4)$$

Where A is a constant, E_g is the band gap of the material and the exponent 'r' depends on the type of transition. Now above equation 4 may be written as

$$\frac{d\left[\ln\left(\alpha h\nu\right)\right]}{d\left(h\nu\right)} = \frac{r}{\left(h\nu - E_g\right)} \quad (5)$$

This indicates that the plot of d[ln(αhυ)]/d(hυ)→ hυ must have a divergence at an energy equal to Eg, where the transition takes place.

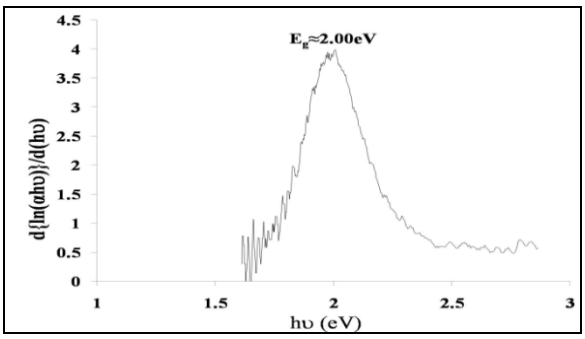

Figure-5
Plot of d{ln(αhυ)}/d(hυ) vs hυ for prepared SnSe nanoparticles

Figure-5 shows the plot of d{ln(αhυ)}/d(hυ) →hυ where a discontinuity at 2.00 eV is clearly observed.

Taking this value as the initial optical band gap of SnSe nanoparticles, ln (αhυ) vs ln (hυ – Eg) graph is plotted to determine the nature of the transition i.e. r value.

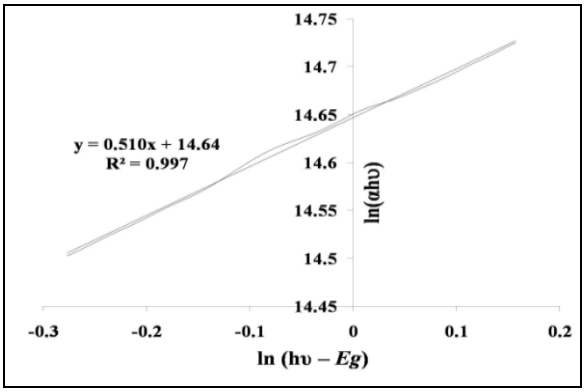

Figure 6
Plot of ln (αhυ) vs ln (hυ – Eg) for prepared SnSe nanoparticles

From the slope of this straight line of figure-6, value of r is found to be 0.510 indicating that the transition is of direct allowed type. Using this value of r (i.e. ~ 0.5), the exact value of the band gap is found out by extrapolating the straight line portion of the $(\alpha h\upsilon)^{1/r}$ → hυ graph to the hυ axis as shown in figure-7.

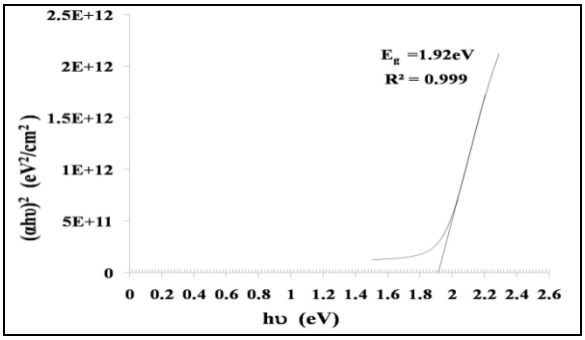

Figure-7
Plot of (αhυ)2 vs hυ for prepared SnSe nanoparticles

The precise value of the optical band gap is found to be 1.92 eV. It is observed that the value of E_g is higher than that of the bulk SnSe (1.1eV) due to quantum confinement in the SnSe nanoparticle. Thus, from the blue-shift of the band gap (E_g), we can calculate the average diameter of the particles using the relation[25,26].

$$\Delta E_g = E_{shift} = \frac{\hbar^2 \pi^2}{2\mu\mu^2} \quad (6)$$

Here E_{shift} is the shift in band gap value, μ is the translation mass and radius of the nanoparticles is r. Below the strong confinement regime, this formula is most applicable.

We have calculated the diameter of the nano particles using above equation and it is found to be ~ 10.13 nm which is comparable to that obtained from XRD and TEM results as shown in table-2.

Table-2
Average particle size as determined using XRD, UV-VIS-NIR and TEM for prepared SnSe nanoparticles

SnSe Annealing temperature	Particle size (nm)		
	XRD	UV-VIS-NIR	TEM
300°C	9.96	10.13	7.58-11.45

Dielectric: Figure-8 shows the plots of capacitance (C) and dielectric loss (tan δ or D) of SnSe nanoparticles as a function of frequency and temperature. Noticeably, the fall in capacitance is very rapid in the low frequency for all the temperatures.

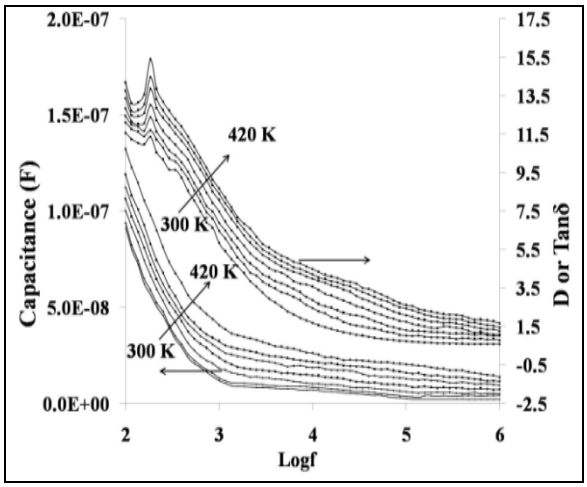

Figure 8
Variation of Capacitance and tanδ or D with temperature and frequency for prepared SnSe nanoparticles

It can be seen that a small peak appears in each spectrum of tanδ vs frequency. This is related to electric relaxation polarization. It is well known fact that due to large surface area of nano structured materials, the surface to volume ratio is very high in comparison to bulk solid. According to Zhang[27] and W. Y. WANG[28], nanostructured materials have about 10^{19} interfaces per cm^3, much more than those of bulk solids. In our experiments, SnSe nanoparticles were compacted under pressure (10MPa) which results in to interfaces with a large volume fraction in the nanostructured sample that contain a large number of defects, such as dangling bonds, vacancies, vacancy clusters and micro porosities. This can cause a change of positive and negative space charge distributions in interfaces which move towards negative and positive poles of the externally applied electric field, respectively. When these charges are trapped by defects, a lot of dipole moments will be generated. Consequently, space-charge polarization occurs in interfaces of SnSe nanoparticles. Because the volume fraction of these interfaces is very large, space-charge polarization plays an important role in the contribution to higher value of C and tanδ for SnSe nanoparticles compared to bulk[29].

Besides this, external electric field rotates these dipoles and rotation direction polarization takes place in interfaces of the SnSe nanoparticles which may be another reason for SnSe nanoparticles to have higher C and tanδ. The dielectric polarization, space-charge polarization and rotation direction polarization appear in the low frequency range and will cause energy loss, so tan δ of SnSe nanoparticles is much higher in low frequency range for all temperature.

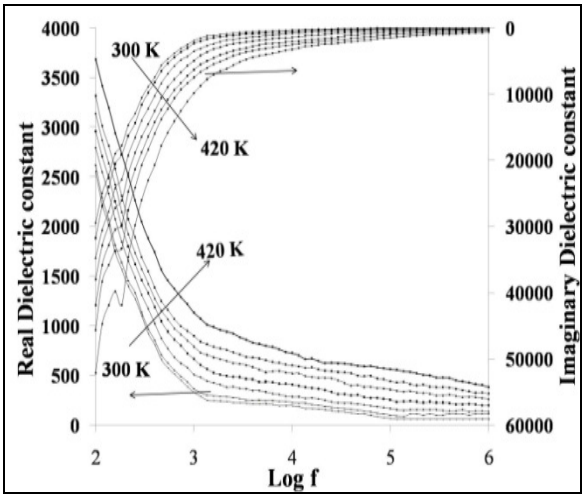

Figure-9
Variation of real (ε') and imaginary (ε'') dielectric constant with temperature and frequency for prepared SnSe nanoparticles

Figure-9 shows the temperature dependent frequency spectra of real and imaginary part of dielectric constant (ε) of SnSe nanoparticles. It can be seen that with the increase of frequency from 100Hz to 1 MHz, ε decreases monotonously. In the low frequency range (from 100Hzto 1 kHz), ε reduces rapidly with the increasing f. After 1 kHz, ε decreases much slowly and remains almost unchanged up to1 MHz.

As mentioned above, due to the interfaces with a large volume fraction, two kinds of polarization (space-charge polarization

and rotation direction polarization) take place in SnSe nanoparticles. However, for bulk materials the number of interfaces is very small and hence both kinds of polarization do not occur. Due this for SnSe nanoparticles we get higher values of ε.

The effect of temperature can be explained using the following relation[29].

$$\tan\delta = \frac{1}{\omega RC} \quad (7)$$

Here resistance (R) of a semiconducting materials decreases with increasing temperature (T) and thus tanδ increases with temperature. It has been pointed out[30] that the influence of temperature on the dielectric constant is strongly attributed to the fact that the increase of lattice defects of the materials at high temperature makes space charge polarization dominant and due to this there is an increase in capacitance, dielectric constant and tanδ with temperature.

Conclusion

In the present paper, we have reported the synthesis of SnSe nanoparticles with average size of ≈15nm by chemical precipitation method in double distilled water as solvent. The small proportion of oxygen has been detected by EDAX which may be incorporated due to environmental processing of aqueous solutions. The nanostructures of the prepared SnSe nanoparticles have been confirmed using XRD, UV-VIS absorption, and TEM. High temperature dielectric properties measurement reveals that capacitance, tanδ or D and dielectric constant strongly depend on frequency and temperature due to polarization, defects and micro porosities present in SnSe nanoparticles.

Acknowledgement

Authors are thankful to UGC, New Delhi for sanctioning major research project.

References

1. W. Dong and C. Zhu, *Opt. Mater,* **22**, 227-233 **(2003)**

2. Yoffe A.D., *Adv. Phys*, **42**, 173-262 **(1993)**

3. Bruce L.E., *J. Chem. Phys.,* **80**, 4403-4409 **(1984)**

4. Zhang Z., Zhao M. and Jiang Q., *Semicond. Sci. Technol*., **16**, L33-L35 **(2001)**

5. Qadri S.B., Skelton E.F., Hsu D., Dinsmore A.D., Yang J., Gray H.F., Ratna B.R., *Phys. Rev. B,* **60**, 9191-9193, **(1999)**

6. Nemec P., Mikes D., Rohovec J., Uhlirova E., Trojanek F. and Maly P., *Mat. Sci. Eng. B,* **69**, 500-504 **(2000)**

7. Suyver J.F., Bakker R., Meijerink A. and Kelly J.J., *Phys. Stat. Sol.(b),* **224**, 307-312 **(2001)**

8. Kelin D.L., Roth R., Lim A.K.L., Alivisatos A.P., McEuen P.L., *Nature,* **389**, 699-701 **(1997)**

9. Murali K.R., Swaminathan V., Trivedi D.C., **81**, 113-118 **(2004)**

10. Zulkarnain Zainal, Saravanan Nagalingam, Anuar kassim, Mohd Zobir Hussein and Wan Mahmood Mat Yunus, *Solar Energy Materials and Solar Cells,* **81**, 261-268, **(2004)**

11. Zweibel K., Solar Energy Mater, *Solar Cells,* **63**, 375-386 **(2000)**

12. L. Seligson and J. Arnold, *J. Amer. Chem. Soc.,* **115**, 8214-8220 **(1993)**

13. Bhatt V.P., Giresan K. and Pandya G.R., *J. Crystal Growth,* **96**, 649-651 **(1989)**

14. Yi H. and Moore J.J., *J. Mater. Sci.,* **25**, 1159-1168 **(1990)**

15. Parkin I.P., *Chem. Soc. Rev*., **25**, 199-207 **(1996)**

16. Subramanian B., Sanjeeviraja C. and Jayachandran M., *J. Crystal Growth*, **234**, 421-426 **(2002)**

17. Wang W., Geng Y., Qian Y., Wang C. and Liu X., *Mater. Res. Bull*., **34**, 403-406 **(1999)**

18. B. Li, Y. Xie, J. Huang and Y. Qian, *Inorg. Chem.,* **39**, 2061-2064 **(2000)**

19. G. Henshaw, I . Parkin and G. Shaw, *J. Chem. Soc. Chem. Commun.,* **10**, 1095-1096 **(1996)**

20. Ziaul Raza Khan, M. Zulfequar, Mohd. Shahid Khan, *Chalcogenide Letters*, **7**, 431-438 **(2010)**

21. M.L. Steigerwald, L.E. Brus, *Acc. Chem. Res.,* **23**, 183 **(1990)**

22. C. Wang, Y.D. Li, G.H. Zhang, J. Zhuang, and G.Q. Shen, *Inorg. Chem.,* **39**, 4237-4239 **(2000)**

23. Zhen Li, Zheng Jiao, Minghong Wu, Qing Liu, Haijian Zhong, Xiang Geng, **40–42**, 313–314 **(2008)**

24. J.I. Pankove, *Optical Processes in Semiconductors*, Englewood Cliffs, NJ: Prentice-Hall, **(1971)**

25. Al. L. Efros, A. L. Efros, *Sov. Phys. Semicond*., **16**, 772-775 **(1982)**

26. W. Wei-Yu, J. N. Schulman, T. Y. Hsu, Feron Uzi, *Appl. Phys. Lett.,* **51**, 710-712 **(1987)**

27. Bin Chen, Jian Sha, Xisheng Ye, Zhengkuanjiao and Lide Zhang, *Science in China,* **42** 510-516 **(1999)**

28. Y.P. Xu, W.Y. Wang, D.F. Zhang, X.L. Chen, **36**, 4401-4403 **(2001)**

29. Samsudi Sakrani, Zulkafli Othaman, Karim Deraman and Yussof Wahab, *J. Fiz. UTM*. , **3**, 99-108 **(2008)**

30. Chopra K.L., Thin Film Phenomena, McGraw-Hill, New York, **(1969)**